Iterative GRAPPA (iGRAPPA) for Improved Parallel Imaging Reconstruction

T. Zhao[1], and X. Hu[1]

[1]Biomedical Engineering, Emory University, Atlanta, GA, United States

Introduction

Partially parallel acquisition techniques have been introduced to accelerate data acquisition for magnetic resonance imaging (1). It was recently shown that the GRAPPA reconstruction could be reformulated as a matrix operator (2). With this formalism, it is possible to reconstruct images directly from the undersampled data without reference lines by calculating the square root of a weight matrix derived from the undersampled data themselves (2, 3). While this is an attractive approach in principle, in practice it is limited by the difficulty in determining the square root of a large matrix and the requirement of special coil configurations. In the present work, an iterative GRAPPA reconstruction method (iGRAPPA), which exploits all acquired lines in addition to the calibration lines in deriving the GRAPPA interpolation weights, is introduced and demonstrated.

Methods

All experiments were carried out on a 3.0 T Siemens Tim MR scanner using a 12-channel head coil. Fully-sampled, multichannel phantom imaging data were obtained using a gradient-echo sequence with the following parameters: TE = 4 ms, TR = 700 ms, matrix size = 128 × 128, field of view (FOV) = 256 × 256 mm2, flip angle = 70º, bandwidth = 460 Hz per pixel, and slice thickness = 5 mm. Data for accelerating factors of 2, 3, and 4 with one calibration block (see Fig. 1 for details) were synthesized by subsampling the fully-sampled data. The reconstruction procedures were performed offline with programs written in MATLAB. The GRAPPA interpolation window is 7 × 4 × 12 (read out × phase encoding × coils).

Fig.1 illustrates the flow diagram of the iGRAPPA algorithm. With calibration lines, the GRAPPA weights are estimated using least squares fitting as usual. The missed lines in Fig.1 can then be filled according to the derived weights. Since GRAPPA kernel holds for any point in the *k*-space, the filled lines can also be used to predict the measured lines, providing a vehicle to improve the accuracy of the weights. Starting from the regular GRAPPA weights, an iterative algorithm as described below is used. At the n^{th} iteration, with the weights determined from previous iteration, the missed lines are first filled accordingly. Using the filled lines to predict the measured lines, new fitting equations are formed by placing the measured data from non-calibration lines on the left side and filled data on the right side of the fitting equation. Combining the new equations with the equations from the calibration lines, the least squares fitting was applied again to generate a new set of weights for the n^{th} iteration. Subsequently, the image at the n^{th} iteration, I_{mn}, was reconstructed using the corresponding weights. A percent change of the n^{th} iteration, F_{pn}, defined according to Eq. [1], was calculated for gauging the convergence. As a regularization step, F_{pn} was forced to be less than $k \times F_{pn-1}$, where k is a regularization parameter ($0 < k < 1$). If this is not the case, the weights of n^{th} iteration, is modified according to Eq.2. Convergence of the iteration was defined as when the percent change reaches a set limit (5 × 10-4 in this study). Two stages are used: **Stage 1.** Using calibration data to obtain the initial weights, followed by iterative GRAPPA reconstruction as shown in Fig.1 with the restriction that only continuously measured lines in the middle of k-space as shown in Fig.1 are used. **Stage 2.** Using weights from Stage 1 as the initial weights, followed by iterative GRAPPA reconstruction as shown in Fig.1 over the entire *k*-space. To compare the performance of GRAPPA and iGRAPPA, the root mean squared (RMS) error between the reconstructed images, Imrecon, and images reconstructed from fully sampled data, Imref, was calculated.

Eq.1 $$Fp_n = \frac{\sum_{all\ pixels} \left| |\mathrm{Im}_n| - |\mathrm{Im}_{n-1}| \right|}{\sum_{all\ pixels} |\mathrm{Im}_{n-1}|}$$

Eq.2 $$W^n_{jr,\ redefined} = (1-p)W^n_{jr} + pW^{n-1}_{jr}, \quad p = k \times Fp_{n-1} / Fp_n$$

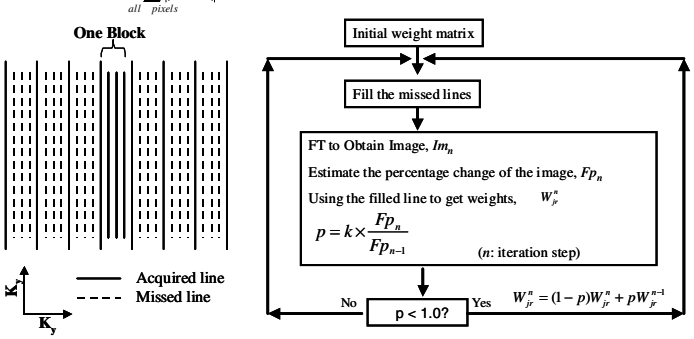

Fig. 1 Schematic k-space acquisition with a 4-fold accelerated factor and the corresponding iGRAPPA reconstruction algorithm.

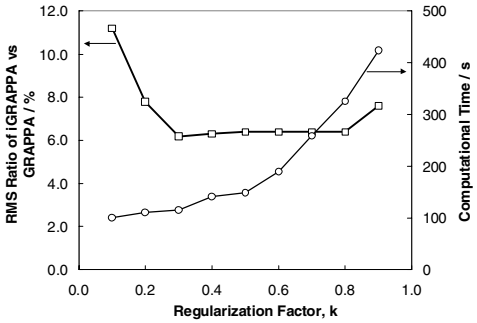

Fig. 2 The influence of the regularization factor, k, on the RMS ratio of iGRAPPA versus GRAPPA and the corresponding computational time.

Results and Discussion

Fig.2 shows the influence of the regularization factor, for the phantom data, on the RMS error ratio of iGRAPPA over GRAPPA and the reconstruction time. Similar reconstructions were obtained for iGRAPPA in a wide range of values for the regularization factor (0.3-0.8), indicating insensitivity to it. However, the computational time of iGRAPPA, i.e. the iteration steps, increases approximately quadratically with the regularization factor.

Fig.3 presents the phantom results of iGRAPPA and GRAPPA on the same data set with acceleration factors of 2 to 4. Minimal calibration lines (one block in Fig.1) were used, which led to considerable ghosting artifacts for GRAPPA reconstruction. In contrast, iGRAPPA significantly reduced the artifacts. For the acceleration factor of 2, 3 and 4, the ratios for iGRAPPA RMS error over that for GRAPPA are 6.40%, 3.89% and 2.96%, respectively, indicating a 10-30 fold reduction in error. Fig.4 illustrates the in vivo results with a 2-fold acceleration factor. The ratio of the RMS errors of iGRAPPA versus GRAPPA is 5.67%, comparable to corresponding phantom results.

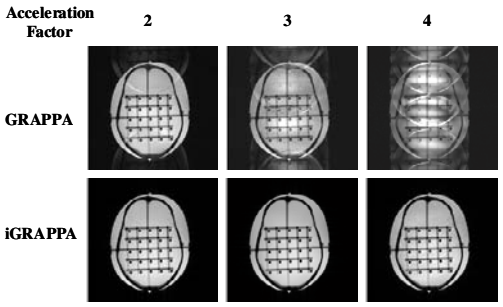

Fig. 3 Phantom results of iGRAPPA versus GRAPPA with difference acceleration factors.

Conclusions

In summary, iGRAPPA, which utilizes all acquired lines in addition to the calibration lines in determining the reconstruction weights, was introduced and demonstrated using both phantom and in vivo data. Compared to GRAPPA, iGRAPPA provides images with significantly reduced parallel imaging artifacts and allows high-quality imaging reconstruction with a smaller number of calibration lines.

Acknowledgements: This work was supported in part by the National Institutes of Health (RO1EB002009) and Georgia Research Alliance.

References

[1] Blaimer M., *et al.*, Top Magn Reson Imaging 2004; **15**:223-236. [2] Griswold M. A., *et al.*, Magn Reson Med 2005; **54**:1553-1556.
[3] Blaimer M. et al., Proc. ISMRM 2006; **12**: 2417.